AIAA JOURNAL
Vol. 38, No. 10, October 2000

Nonlinear Behavior of Thick Composites with Uniform Fiber Waviness

Heoung-Jae Chun* and Jai-Yoon Shin†
Yonsei University, Seoul 120-749, Republic of Korea
and
Isaac M. Daniel‡
Northwestern University, Evanston, Illinois 60208

A constitutive model was proposed to study the effects of fiber waviness on the elastic properties and nonlinear behavior of unidirectional composites under tensile, compressive, and flexural loadings. The material and geometric nonlinearities due to fiber waviness were incorporated in the analyses. Specimens with various degrees of fiber waviness were fabricated. Tensile, compressive, and flexural tests were conducted to verify the predictions obtained from the model. Experimental results were in good agreement with the predictions.

Nomenclature

$\overline{A_{ij}}, \overline{B_{ij}}, \overline{D_{ij}}$ = average stiffnesses of a representative volume element
$\overline{a_{ij}}, \overline{b_{ij}}, \overline{c_{ij}}, \overline{d_{ij}}$ = average compliances of a representative volume element
a_l = amplitude of fiber waviness in the lth thin slice
$\overline{a^d_{xx}}, \overline{b^d_{xx}}, \overline{d^d_{xx}}$ = differential compliances of a representative volume element
$(C^{**}_{pq})_l$ = off-axis stiffnesses of an infinitesimally short subelement of the lth thin slice
$\mathrm{d}S_l, S_l$ = fiber length in an infinitesimally short subelement and fiber length in the lth thin slice
$E_x, (\overline{E^{d***}_x})_l$ = Young's modulus and tangential Young's modulus in the lth thin slice
h = laminate thickness
N, M = force and moment resultants
Q^{e**}_{ij} = plane-stress moduli neglecting the higher-order stress terms
$(Q^{**}_{ij})_l$ = plane-stress moduli of an infinitesimally short subelement of the lth thin slice
$[R]$ = Reuter matrix
$S_{ij}, S_{iii}, S_{iiii}$ = compliances
$[S^*], S^*_{ij}$ = on-axis compliance matrix and elements
$[S^{**}]$ = off-axis compliance matrix
$[S^{***}]$ = off-axis compliance matrix under x-direction loading
$(\overline{S^{***}_{ij}})_c$ = average compliances for a representative volume element
$[(\overline{S^{***}})_l], (\overline{S^{***}_{ij}})_l$ = average compliance matrix and elements in the lth thin slice
$[T]$ = transformation matrix
W^* = complementary energy density function
z_l = distance from the midplane to the lth thin slice
$\Delta\varepsilon_{xx}, (\Delta\varepsilon_{xx})_l$ = incremental strain along x direction
$(\Delta\overline{\varepsilon_f})_l$ = incremental average fiber strain in the lth thin slice
$\Delta\kappa_{xx}$ = incremental curvature in a representative volume element
$(\Delta\sigma_{xx})_l$ = incremental stress in x direction for the lth thin slice
$\varepsilon_{ij}, [\varepsilon]_{1,2,3}, [\varepsilon]_{x,y,z}$ = strains
$(\varepsilon_f)_l, (\overline{\varepsilon_f})_l$ = fiber strain of an infinitesimally short subelement and average fiber strain in the lth thin slice
$[(\varepsilon)_l]_{x,y,z}$ = strain in the lth thin slice
ε^0 = effective middle surface extensional strain in a representative volume element
$[\varepsilon^0]_s$ = middle surface extensional strain of an infinitesimally short subelement
θ, θ_l = angle between the tangent to the fiber and x axis
κ = effective curvature in a representative volume element
$[\kappa]_s$ = overall laminate curvature of an infinitesimally short subelement
λ_l = wavelength of fiber waviness in the lth thin slice
ν_{xy} = Poisson's ratio
$\sigma_{ij}, [\sigma]_{1,2,3}, [\sigma]_{x,y,z}$ = stresses
$[(\sigma)_l]_{x,y,z}$ = stress in the lth thin slice
τ_{ij} = shear stresses

Introduction

FIBER waviness is one of the manufacturing defects frequently encountered in thick composite structures. It results from local buckling of prepregs, or from wet hoop-wound filament strands under the pressure exerted by the overwrapped layers during the filament winding process, or from lamination residual stresses built up during curing. Its characteristics can be represented by the thickness undulation of fibers within a thick composite laminate.

A number of studies have been conducted on the behavior of thick composites with fiber waviness. Shuart[1] considered both in-plane and out-of-plane fiber waviness in a microbuckling model for multidirectional laminates. Bogetti et al.[2] applied laminated plate theory to a model to predict stiffness and strength reduction due to layer waviness. Telegadas and Hyer[3] conducted finite element analyses on composites with fiber waviness. Chou and Takahashi[4] predicted the tensile stress–strain response of flexible wavy fiber composites. Hsiao and Daniel[5–7] investigated the effect of fiber waviness on compressive behavior of thick composites. However, integrated studies of the effects of fiber waviness on nonlinear behavior of unidirectional composites under various loadings have not been conducted.

Received 11 June 1999; revision received 15 January 2000; accepted for publication 21 February 2000.

*Assistant Professor, School of Electrical and Mechanical Engineering, 134 Shinchon-Dong, Seodaemun-Ku.
†Graduate Student, Department of Mechanical Engineering, 134 Shinchon-Dong, Seodaemun-Ku.
‡Professor, Departments of Mechanical and Civil Engineering.

In this study, the nonlinear behavior of thick composites with fiber waviness was investigated theoretically and experimentally under tensile, compressive, and flexural loadings.

Analysis

Unidirectional composites examined are composed of continuous fibers with sinusoidal waviness in a matrix. Because of material as well as geometric factors, the mechanical behavior of these composites is generally nonlinear under finite deformation. A constitutive model is proposed for predicting the elastic properties and nonlinear behavior of composites with fiber waviness. Uniform fiber waviness is assumed in the analysis.

Figure 1 shows a representative volume element encompassing one period of uniform fiber waviness. It is assumed that all fibers are parallel to each other and have sinusoidal curvature along one coordinate direction (x axis). The representative volume element is then divided into thin slices along the thickness direction (z axis). Then each thin slice can be considered as a thin ply with varying fiber orientation along the x axis. Each infinitesimally short subelement in each thin slice can be treated as an off-axis unidirectional lamina.

For the lth thin slice, the fiber orientation is given by

$$\theta_l = \tan^{-1}[(2\pi a_l/\lambda_l)\cos(2\pi x/\lambda_l)] \tag{1}$$

The complementary energy density function W^* is used to incorporate the material nonlinearity in the model. For nonlinear elastic composites, the fourth-order expansion of W^* is considered:

$$\begin{aligned} W^* = {} & \tfrac{1}{2}S_{11}\sigma_{11}^2 + \tfrac{1}{2}S_{22}\sigma_{22}^2 + \tfrac{1}{2}S_{33}\sigma_{33}^2 + \tfrac{1}{2}S_{44}\tau_{23}^2 + \tfrac{1}{2}S_{55}\tau_{13}^2 \\ & + \tfrac{1}{2}S_{66}\tau_{12}^2 + \tfrac{1}{3}S_{111}\sigma_{11}^3 + \tfrac{1}{3}S_{222}\sigma_{22}^3 + \tfrac{1}{3}S_{333}\sigma_{33}^3 + \tfrac{1}{4}S_{1111}\sigma_{11}^4 \\ & + \tfrac{1}{4}S_{2222}\sigma_{22}^4 + \tfrac{1}{4}S_{3333}\sigma_{33}^4 + \tfrac{1}{4}S_{4444}\tau_{23}^4 + \tfrac{1}{4}S_{5555}\tau_{13}^4 \\ & + \tfrac{1}{4}S_{6666}\tau_{12}^4 + S_{12}\sigma_{11}\sigma_{22} + S_{13}\sigma_{11}\sigma_{33} + S_{23}\sigma_{22}\sigma_{33} \end{aligned} \tag{2}$$

The strain–stress relations can be derived from the complementary energy density as follows:

$$\varepsilon_{ij} = \frac{\partial W^*}{\partial \sigma_{ij}} \tag{3}$$

where $i, j = 1, 2, 3, 4, 5, 6$ in contracted notation. If the nonlinear coupling terms between normal and shear stresses are neglected, the strain–stress relations referred to material coordinates can be expressed in the following matrix form:

$$[\varepsilon]_{1,2,3} = [S^*][\sigma]_{1,2,3} \tag{4}$$

where the corresponding compliances are expressed as follows:

$$\begin{aligned} S_{11}^* &= S_{11} + S_{111}\sigma_{11} + S_{1111}\sigma_{11}^2 \\ S_{22}^* &= S_{22} + S_{222}\sigma_{22} + S_{2222}\sigma_{22}^2 \\ S_{33}^* &= S_{33} + S_{333}\sigma_{33} + S_{3333}\sigma_{33}^2 \\ S_{44}^* &= S_{44} + S_{4444}\tau_{23}^2, \qquad S_{55}^* = S_{55} + S_{5555}\tau_{13}^2 \\ S_{66}^* &= S_{66} + S_{6666}\tau_{12}^2, \qquad S_{12}^* = S_{21}^* = S_{12} \\ S_{13}^* &= S_{31}^* = S_{13}, \qquad S_{23}^* = S_{32}^* = S_{23} \end{aligned}$$

For composites with off-axis fiber orientation on the x–z plane, the strain–stress relations referred to the loading coordinates can be obtained by using the following transformation relation:

$$[\varepsilon]_{x,y,z} = [R][T]^{-1}[R]^{-1}[S^*][T][\sigma]_{x,y,z} = [S^{**}][\sigma]_{x,y,z} \tag{5}$$

where

$$[T] = \begin{bmatrix} m^2 & 0 & n^2 & 0 & 2mn & 0 \\ 0 & 1 & 0 & 0 & 0 & 0 \\ n^2 & 0 & m^2 & 0 & -2mn & 0 \\ 0 & 0 & 0 & m & 0 & -n \\ -mn & 0 & mn & 0 & m^2 - n^2 & 0 \\ 0 & 0 & 0 & n & 0 & m \end{bmatrix}$$

$$[R] = \begin{bmatrix} 1 & 0 & 0 & 0 & 0 & 0 \\ 0 & 1 & 0 & 0 & 0 & 0 \\ 0 & 0 & 1 & 0 & 0 & 0 \\ 0 & 0 & 0 & 2 & 0 & 0 \\ 0 & 0 & 0 & 0 & 2 & 0 \\ 0 & 0 & 0 & 0 & 0 & 2 \end{bmatrix}$$

where $m = \cos\theta$ and $n = \sin\theta$.

For composites under tensile, compressive, and constant flexural loadings, it is reasonable to assume that the loadings cause only normal stress in the longitudinal direction. Therefore, all other components of normal and shear stress are zero. For a particular thin slice, the stress components in the material coordinates for the infinitesimally short subelement are obtained by coordinate transformation as

$$\begin{aligned} \sigma_{11} = m^2\sigma_{xx}, \qquad \sigma_{33} = n^2\sigma_{xx}, \qquad \tau_{13} = -mn\sigma_{xx} \\ \sigma_{22} = \tau_{23} = \tau_{12} = 0 \end{aligned} \tag{6}$$

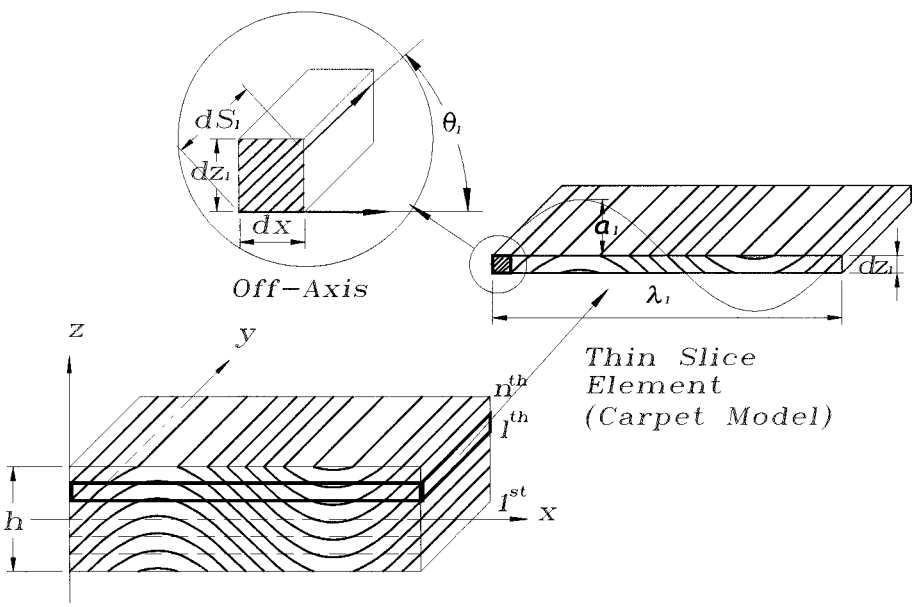

Fig. 1 Schematic drawing of a representative volume element and coordinates for unidirectional composite with uniform fiber waviness.

From these relations, the strain–stress relations, Eq. (5), for composite materials with out-of-plane fiber orientation are reduced to the following:

$$[\varepsilon]_{x,y,z} = [S^{***}][\sigma]_{x,y,z} \tag{7}$$

The lengthwise average strain–stress relations for each thin slice are obtained by integrating the transformed compliances over a period of waviness:

$$[(\varepsilon)_l]_{x,y,z} = \left[(\overline{S^{***}})_l\right][(\sigma)_l]_{x,y,z} \tag{8}$$

where

$$\left(\overline{S_{ij}^{***}}\right)_l = \frac{1}{\lambda_l}\int_0^{\lambda_l} \left(S_{ij}^{***}\right)_l \mathrm{d}x$$

The average compliances for a representative volume element are obtained by summing the effects of all thin slices:

$$\left(\overline{S_{ij}^{***}}\right)_c = \frac{1}{h}\sum_l \left(\overline{S_{ij}^{***}}\right)_l \mathrm{d}z = \frac{1}{h}\int_{-h/2}^{h/2} \overline{S_{ij}^{***}}\,\mathrm{d}z \tag{9}$$

The effective elastic properties for composites with fiber waviness are obtained by the following relations after dropping the compliance terms of higher order:

$$E_x = 1\Big/\left(\overline{S_{11}^{***}}\right)_c, \qquad \nu_{xy} = -\left[\left(\overline{S_{21}^{***}}\right)_c\Big/\left(\overline{S_{11}^{***}}\right)_c\right] \tag{10}$$

If the lateral dimensions (x–y plane) of the composite material are much larger than its thickness (z direction) and the laminate is loaded only in this plane (x–y plane), it is reasonable to adopt the classical lamination theory. Stresses in the short subelement at a distantce z_l from the midplane are expressed in terms of the middle surface extensional strain $[\varepsilon^0]_s$ and overall laminate curvature $[\kappa]_s$ as follows:

$$\begin{bmatrix}(\sigma_{xx})_l\\(\sigma_{yy})_l\\(\tau_{xy})_l\end{bmatrix}_s = \begin{bmatrix}\left(Q_{xx}^{**}\right)_l & \left(Q_{xy}^{**}\right)_l & 0\\ \left(Q_{yx}^{**}\right)_l & \left(Q_{yy}^{**}\right)_l & 0\\ 0 & 0 & \left(Q_{ss}^{**}\right)_l\end{bmatrix}_s \begin{bmatrix}\varepsilon_{xx}^0\\ \varepsilon_{yy}^0\\ \tau_{xy}^0\end{bmatrix}_s + z_l \begin{bmatrix}\left(Q_{xx}^{**}\right)_l & \left(Q_{xy}^{**}\right)_l & 0\\ \left(Q_{yx}^{**}\right)_l & \left(Q_{yy}^{**}\right)_l & 0\\ 0 & 0 & \left(Q_{ss}^{**}\right)_l\end{bmatrix}_s \begin{bmatrix}\kappa_{xx}\\ \kappa_{yy}\\ \kappa_{xy}\end{bmatrix}_s \tag{11}$$

where $(Q_{ij}^{**})_l$ are plane-stress moduli calculated from off-axis stiffnesses $(C_{pq}^{**})_l$ and $[(C^{**})_l]_s = [(S^{**})_l]_s^{-1}$ and are given in Appendix A. The resultant forces N and moments M for a representative volume element are obtained by integrating the effects for all infinitesimally short subelements and stiffness over a period of wavelength. Thus, the force and moment resultants are obtained as follows:

$$\begin{bmatrix}N\\ -\\ M\end{bmatrix} = \begin{bmatrix}\bar{A}\,|\,\bar{B}\\ -\;-\\ \bar{B}\,|\,\bar{D}\end{bmatrix}\begin{bmatrix}\varepsilon^0\\ -\\ \kappa\end{bmatrix} \tag{12}$$

where

$$\overline{A_{ij}} = \frac{1}{\lambda_l}\int_0^{\lambda_l}\int_{-h/2}^{h/2} Q_{ij}^{**}\,\mathrm{d}z\,\mathrm{d}x, \qquad \overline{B_{ij}} = \frac{1}{\lambda_l}\int_0^{\lambda_l}\int_{-h/2}^{h/2} z\,Q_{ij}^{**}\,\mathrm{d}z\,\mathrm{d}x$$

$$\overline{D_{ij}} = \frac{1}{\lambda_l}\int_0^{\lambda_l}\int_{-h/2}^{h/2} z^2 Q_{ij}^{**}\,\mathrm{d}z\,\mathrm{d}x$$

The effective flexural properties for composite material with fiber waviness are obtained from the following relations:

$$\overline{D_{ij}} = \frac{1}{\lambda_l}\int_0^{\lambda_l}\int_{-h/2}^{h/2} z^2 Q_{ij}^{e^{**}}\,\mathrm{d}z\,\mathrm{d}x \tag{13}$$

where $[Q_{ij}^{e^{**}}]$ are obtained from $[Q_{ij}^{**}]$ in Eq. (11) by dropping the compliance terms of higher order.

Equation (12) can be expressed in the alternate form through matrix inversion:

$$\begin{bmatrix}\varepsilon^0\\ -\\ \kappa\end{bmatrix} = \begin{bmatrix}\bar{a}\,|\,\bar{b}\\ -\;-\\ \bar{c}\,|\,\bar{d}\end{bmatrix}\begin{bmatrix}N\\ -\\ M\end{bmatrix} \tag{14}$$

where

$$[\bar{a}] = [\bar{A}]^{-1} + [\bar{A}]^{-1}[\bar{B}]([\bar{D}] - [\bar{B}][\bar{A}]^{-1}[\bar{B}])^{-1}[\bar{B}][\bar{A}]^{-1}$$

$$[\bar{b}] = -[\bar{A}]^{-1}[\bar{B}]([\bar{D}] - [\bar{B}][\bar{A}]^{-1}[\bar{B}])^{-1}$$

$$[\bar{c}] = -([\bar{D}] - [\bar{B}][\bar{A}]^{-1}[\bar{B}])^{-1}[\bar{B}][\bar{A}]^{-1}$$

$$[\bar{d}] = ([\bar{D}] - [\bar{B}][\bar{A}]^{-1}[\bar{B}])^{-1}$$

Geometric nonlinearity is introduced when the shape of fiber waviness in a representative volume element is changed during loading. The fiber length $\mathrm{d}S_l$ in an infinitesimally short subelement of length $\mathrm{d}x$ of the lth thin slice is obtained as

$$\mathrm{d}S_l = \sqrt{\mathrm{d}x^2 + \mathrm{d}x^2\tan^2\theta_l} \tag{15}$$

The total length of fiber in one period of waviness of the lth thin slice is obtained as follows using the elliptic integral of the second kind:

$$S_l = \int_0^{\lambda}\mathrm{d}S_l = \frac{\lambda_l}{2\pi}\frac{1}{\sqrt{1-k_l^2}}\int_0^{2\pi}\sqrt{1-k_l\sin^2\beta}\,\mathrm{d}\beta$$

$$= \lambda_l\left[1 + 2\left(\frac{k_l^2}{8}\right) + 13\left(\frac{k_l^2}{8}\right)^2 + 90\left(\frac{k_l^2}{8}\right)^3 + \cdots\right] \tag{16}$$

where $c_l = (2\pi a_l/\lambda_l)^2$ and $k_l^2 = c_l/(c_l+1)$.

Because k_l is smaller than 1, this series converges. The strain in the fiber direction of an infinitesimally short subelement is given in terms of strains along the loading coordinates by

$$(\varepsilon_f)_l = \cos^2\theta_l(\varepsilon_{xx})_l + \sin^2\theta_l(\varepsilon_{zz})_l + \sin\theta_l\cos\theta_l(\gamma_{xz})_l \tag{17}$$

The average fiber strain in the lth thin slice along the fiber direction is obtained as

$$(\overline{\varepsilon_f})_l = \frac{1}{S_l}\int_0^{S_l}\cos^2\theta_l(\varepsilon_{xx})_l + \sin^2\theta_l(\varepsilon_{zz})_l + \sin\theta_l\cos\theta_l(\gamma_{xz})_l\,\mathrm{d}S_l$$

$$= \left\{\left(\overline{S_{13}^{***}}\right)_l + \left[\left(\overline{S_{11}^{***}}\right)_l - \left(\overline{S_{13}^{***}}\right)_l\right]F(k_l)\right\}(\sigma_{xx})_l \tag{18}$$

where

$$F(k_l) = \frac{1}{S_l}\int_0^{S_l}\cos^2\theta_l\,\mathrm{d}S_l = \left(1-k_l^2\right)\left(1 + \frac{1}{4}k_l^2 + \frac{9}{64}k_l^4 + \frac{50}{512}k_l^6 + \frac{1225}{16{,}384}k_l^8 + \frac{3969}{65{,}536}k_l^{10} + \cdots\right)\Big/\left(1 - \frac{1}{4}k_l^2 - \frac{3}{64}k_l^4 - \frac{10}{512}k_l^6 - \frac{175}{16{,}384}k_l^8 - \frac{441}{65{,}536}k_l^{10} + \cdots\right)$$

The incremental method is adopted together with the change of strains in the fiber direction to examine the geometric nonlinearity associated with deformation. If the material is subjected to monotonic tensile or compressive loading N_{xx} in the x direction, the incremental strain of the lth thin slice in the loading direction is obtained as

$$(\Delta\varepsilon_{xx})_l = \overline{a_{xx}^d}\,\Delta N_{xx} \tag{19}$$

where $\overline{a_{xx}^d}$ is the differential compliance obtained by substituting $2\sigma_{xx}$ for σ_{xx} and $3\sigma_{xx}^2$ for σ_{xx}^2 in Eq. (7) and following the procedures in Eqs. (11–14). For the case of bending loading, a moment component perpendicular to the x–z plane, M_{xx}, is applied to the composite material. The incremental strain $\Delta\varepsilon_{xx}$ and curvature $\Delta\kappa_{xx}$ for the given incremental bending moment in the lth thin slice are obtained as

$$(\Delta\varepsilon_{xx})_l = \left(\overline{b_{xx}^d} + \overline{d_{xx}^d}z_l\right)\Delta M_{xx} \tag{20a}$$

$$\Delta\kappa_{xx} = \overline{d_{xx}^d}\,\Delta M_{xx} \tag{20b}$$

where $\overline{b^d_{xx}}$ and $\overline{d^d_{xx}}$ are the differential compliances obtained by similar procedures as used for obtaining $\overline{a^d_{xx}}$. The corresponding incremental stress in the loading direction for the lth thin slice is obtained from

$$(\Delta\sigma_{xx})_l = \left(\overline{E_x^{d***}}\right)_l (\Delta\varepsilon_{xx})_l \tag{21}$$

where $(\overline{E_x^{d***}})_l$ is given in Appendix B.

The average strain increment of the fiber in the lth thin slice for an applied uniaxial stress in the x direction is given by

$$(\Delta\overline{\varepsilon_f})_l = \left\{\left[\left(\overline{S_{11}^{d***}}\right)_l - \left(\overline{S_{13}^{d***}}\right)_l\right]F(k_l) + \left(\overline{S_{13}^{d***}}\right)_l\right\}(\Delta\sigma_{xx})_l \tag{22}$$

where $(\overline{S_{11}^{d***}})_l$ and $(\overline{S_{13}^{d***}})_l$ are given in Appendix B.

The current stresses and strains are determined when the rth increments are added to the earlier state of stress and strain as follows:

$$[(\sigma_{xx})_l]_r = \sum_{i=1}^{r}[(\Delta\sigma_{xx})_l]_i \tag{23a}$$

$$[(\varepsilon_{xx})_l]_r = \exp\left\{\sum_{i=1}^{r}[(\Delta\varepsilon_{xx})_l]_i\right\} - 1 \tag{23b}$$

$$[(\overline{\varepsilon_f})_l]_r = \exp\left\{\sum_{i=1}^{r}[(\Delta\overline{\varepsilon_f})_l]_i\right\} - 1 \tag{23c}$$

The changed wavelength and length of the fiber in the lth thin slice are calculated from these strains as follows:

$$(\lambda_l)_r = (\lambda_l)_0\{1 + [(\varepsilon_{xx})_l]_r\} \tag{24a}$$

$$(S_l)_r = (S_l)_0\{1 + [(\overline{\varepsilon_f})_l]_r\} \tag{24b}$$

To determine the change of shape of fiber waviness during the load increment, it is assumed that the fibers in each thin slice maintain a similar sinusoidal shape of waviness while varying only in their amplitude a_l and wavelength λ_l. The amplitude of waviness in the thin slice for the rth step loading is determined by Eqs. (16) and (24) using the Newton–Raphson method. From these newly determined values of amplitude $(a_l)_r$ and changed wavelength $(\lambda_l)_r$ from Eq. (24a), the changed angle $(\theta_l)_r$ between the tangent to the fiber and x axis is obtained from Eq. (1). With this changed angle, calculations from Eqs. (16–24) are repeated for the $(r + 1)$th step of loading. These repeated procedures continue till the final value of loading is reached.

Experimental Procedures

The material investigated in this study was DMS 2224 graphite/epoxy composite material (Hexcel, Inc.). Tensile and compressive tests were conducted, in an MTS servo-hydraulic testing machine, with the standard composite coupons without fiber waviness to obtain the elastic properties and higher order compliances. The IITRI compression test fixture was used in the experiments for compressive loading.

A special fabrication technique was developed for producing thick composites plates with controlled uniform fiber waviness. Molds with various sinusoidal wave shapes were used to fabricate the composite plates with fiber waviness in an autoclave following a special two-step curing cycle.[8] Specimens with three waviness ratios (amplitude/wavelength) with a wavelength of 20 mm were obtained from the fabricated plates. The fiber waviness ratios were 0.011, 0.034, and 0.059. The test coupons were 150 mm long and 10 mm wide with various thicknesses ranging between 5.2 and 10 mm.

The test coupons were instrumented with commercially available strain gauges (EA and CA gauges from Measurements Group, Inc.) for measuring longitudinal and transverse strains. The strain gauges were bonded on the specimen surfaces with M-Bond 200 (Measurements Group, Inc.). The strain gauge outputs were conditioned and amplified through a dynamic strain bridge conditioner and amplifier (Shinkoh, Inc.) and recorded by a data acquisition system installed in the control system (MTS Test Star II). The acquired data were transferred to a personal computer and stored on a hard disk. A four-point-bending test fixture was designed and fabricated to conduct flexural tests. Geometries of four-point-bending coupons are shown in Fig. 2. The deflection at the center of the span of the composite specimen was measured with a homemade displacement transducer because the composite material was loaded under pure bending in that section. Tensile, compressive, and four-point-bending tests were conducted while monitoring the deflections, strains, and applied loads.

Table 1 Mechanical properties of DMS 2224 graphite/epoxy composite

Property	Value
Tensile longitudinal modulus E_{1t}, GPa	120
Tensile transverse modulus E_{2t}, GPa	9.07
In-plane shear modulus G_{12}, GPa	4.73
Tensile major Poisson's ratio ν_{12t}	0.286
Tensile minor Poisson's ratio ν_{21t}	0.022
Compressive longitudinal modulus E_{1c}, GPa	122
Compressive transverse modulus E_{2c}, GPa	9.11
Compressive major Poisson's ratio ν_{12c}	0.293
Compressive minor Poisson's ratio ν_{21c}	0.022

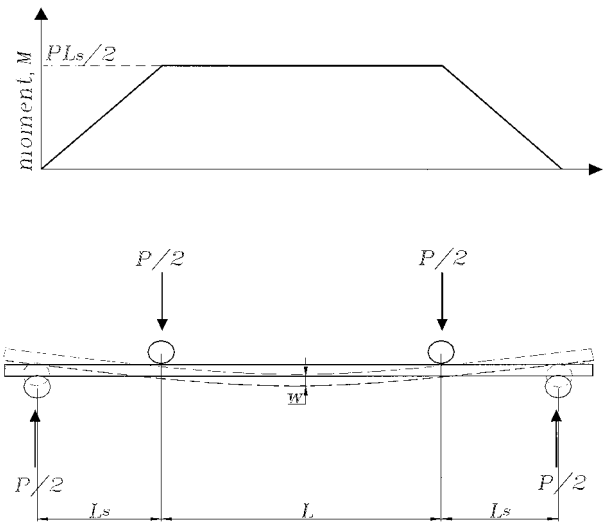

Fig. 2 Schematic drawing of four-point-bending test geometries.

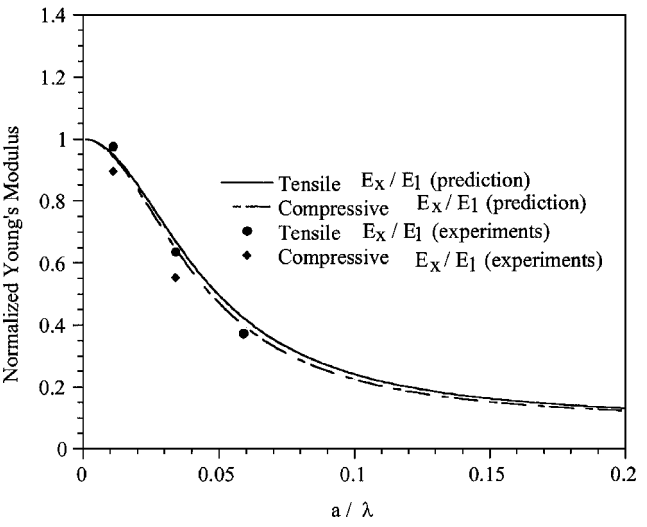

Fig. 3 Predicted and experimentally obtained normalized Young's moduli as a function of fiber waviness ratio for the uniform fiber waviness model.

Results and Discussion

The mechanical properties and higher-order compliances for material nonlinearity were obtained from tensile and compressive stress–strain curves and are listed in Tables 1 and 2, respectively.

Figure 3 shows the comparison between the predictions and the experimental results for the normalized Young's modulus (E_x/E_l) as a function of fiber waviness ratio for the uniform fiber waviness model. It is seen from Fig. 3 that a significant reduction of

Table 2 Compliances of DMS 2224 graphite/epoxy composite

Compliances	Values	Compliances	Values
S_{11t}, GPa^{-1}	0.008333	S_{11c}, GPa^{-1}	0.008217
S_{111t}, GPa^{-2}	−0.0003361	S_{111c}, GPa^{-2}	−0.0005383
S_{1111t}, GPa^{-3}	0.00005745	S_{1111c}, GPa^{-3}	0.0007787
$S_{33t}(S_{22t})$, GPa^{-1}	0.1102	$S_{33c}(S_{22c})$, GPa^{-1}	0.1097
$S_{333t}(S_{222t})$, GPa^{-2}	−0.02610	$S_{333c}(S_{222c})$, GPa^{-2}	0.1186
$S_{3333t}(S_{2222t})$, GPa^{-3}	1.580	$S_{3333c}(S_{2222c})$, GPa^{-3}	1.476
$S_{13t}(S_{12t})$, GPa^{-1}	−0.002384	$S_{13c}(S_{12c})$, GPa^{-1}	−0.002415
S_{23t}, GPa^{-1}	−0.04188	S_{23c}, GPa^{-1}	−0.04171
$S_{66t}(S_{55t})$, GPa^{-1}	0.2115	$S_{66c}(S_{55c})$, GPa^{-1}	0.2294
$S_{6666t}(S_{5555t})$, GPa^{-3}	50.13	$S_{6666c}(S_{5555c})$, GPa^{-3}	17.18

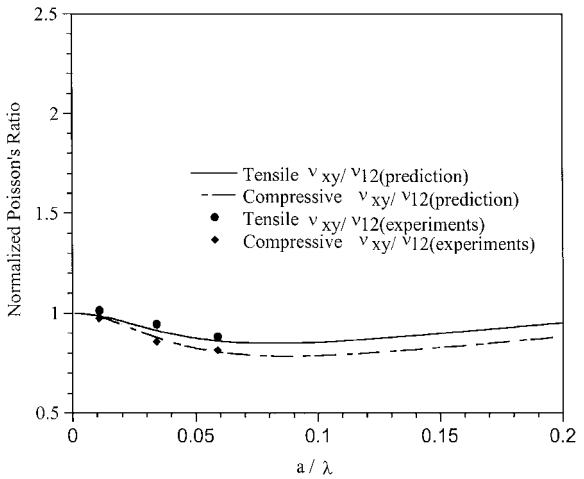

Fig. 4 Predicted and experimentally obtained normalized Poisson's ratios as a function of fiber waviness ratio for the uniform fiber waviness model.

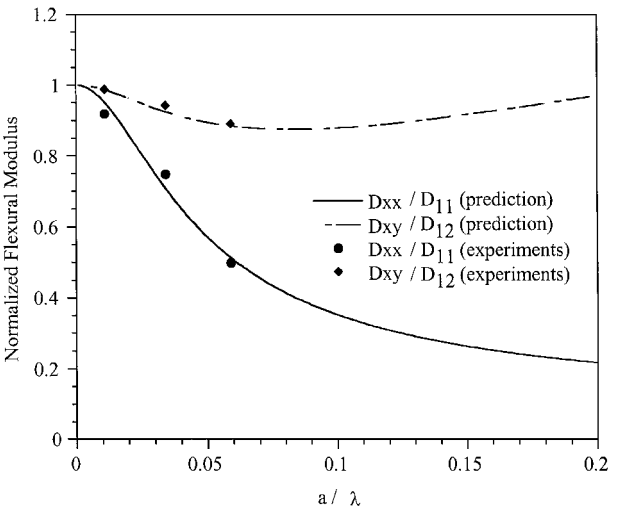

Fig. 5 Predicted and experimentally obtained flexural stiffnesses as a function of fiber waviness ratio for the uniform fiber waviness model.

Young's modulus is observed as the fiber waviness ratio increases. The rate of reduction for E_x increases up to a fiber waviness ratio of 0.04, then, decreases gradually. Figure 4 shows the comparison between the predictions and the experimental results for the normalized Poisson's ratio (ν_{xy}/ν_{12}) as a function of fiber waviness ratio for the uniform fiber waviness model. As shown in Fig. 4, ν_{xy} decreases up to a fiber waviness ratio of 0.08 and then increases after that value. Figure 5 shows comparisons between the predictions and the experimental results for the normalized flexural stiffnesses, D_{xx}/D_{11} and D_{xy}/D_{12}, as a function of fiber waviness ratio for the uniform fiber waviness model. It is seen from Fig. 5 that a significant reduction of the flexural modulus D_{xx} is observed as the fiber waviness ratio increases. D_{xy} decreases moderately and increases slightly with fiber waviness ratio. It is observed from Figs. 3–5 that the predicted elastic values are in good agreement with the experimental results.

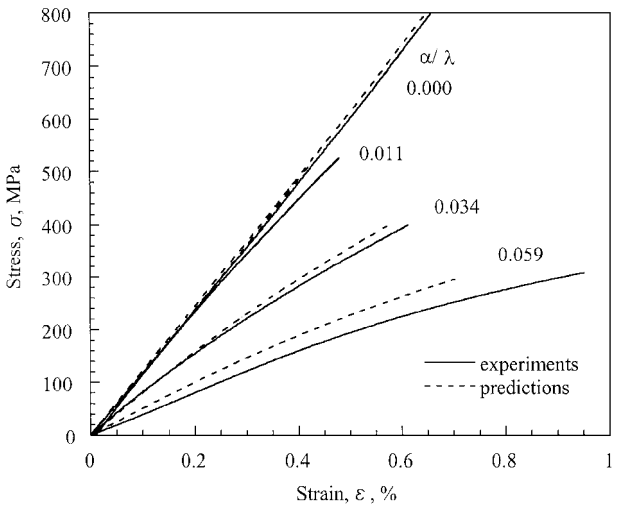

Fig. 6 Predicted and experimentally obtained tensile stress–strain curves for the uniform fiber waviness model with various fiber waviness ratios.

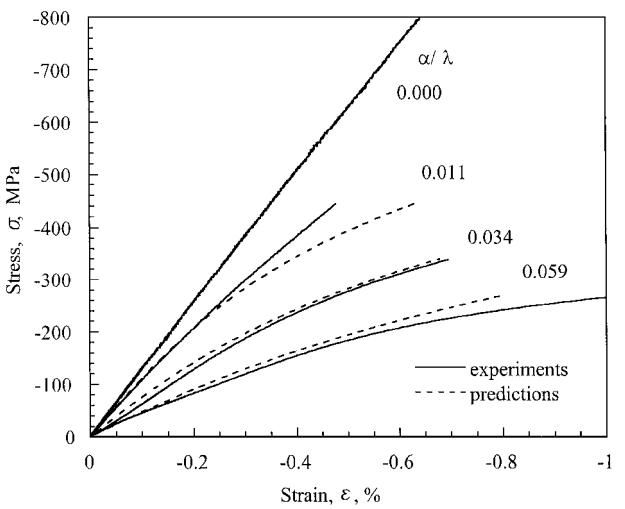

Fig. 7 Predicted and experimentally obtained compressive stress–strain curves for the uniform fiber waviness model with various fiber waviness ratios.

Figures 6 and 7 show comparisons between the predicted and experimentally obtained tensile and compressive stress–strain curves for the uniform fiber waviness model, respectively. It is noted in Figs. 6 and 7 that the tensile as well as the compressive behavior of composites is strongly influenced by the degree of fiber waviness. It is also observed that the strength of the composite material decreases while the ultimate strain increases with increase of fiber waviness ratio, which indicates that the failure of composites is strongly influenced by the degree of fiber waviness. It is shown in Figs. 6 and 7 that the stress–strain curves under tensile loading show more stiffening than those under compressive loading. These results are believed to be associated with the role of geometric nonlinearity due to fiber waviness. The composite coupons with fiber waviness under tensile loading tend to stretch the wavy fibers so that they stiffen during

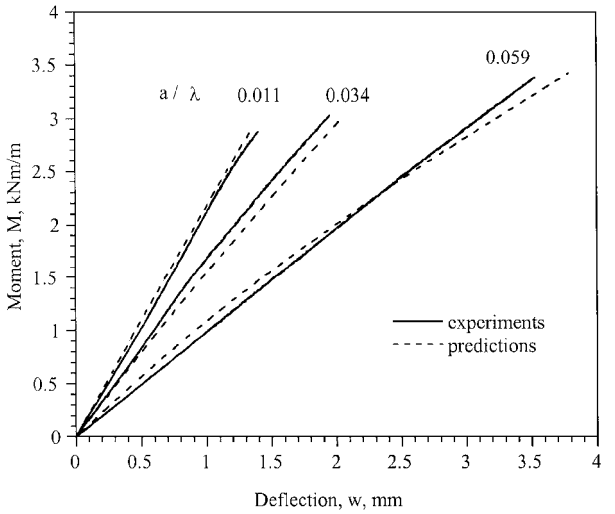

Fig. 8 Predicted and experimentally obtained bending moment-deflection curves for the uniform fiber waviness model with various fiber waviness ratios.

the deformation. However, the coupons under compressive loading tend to undulate the wavy fibers further so that they soften during the deformation. Figure 8 shows the comparison between the predicted and experimentally obtained bending moment-deflection curves for uniform fiber waviness. It is shown that the flexural behavior of the composite material is also strongly influenced by the degree of fiber waviness ratio. The predicted curves are in good agreement with experimental results.

Conclusions

A constitutive model was proposed to study the effects of fiber waviness on nonlinear behavior of composite materials. Elastic tensile, compressive, and flexural properties and behavior of the composites were predicted. The material and geometric nonlinearities due to fiber waviness were incorporated in the analysis.

A special fabrication technique was developed to produce thick composite specimens with controlled uniform fiber waviness ratios.

Mechanical characterization was conducted on the composites to determine the mechanical properties and higher-order compliances for material nonlinearity.

Tensile, compressive, and flexural tests were conducted on specimens with fiber waviness in a servo-hydraulic testing machine while monitoring the applied loads, deflections, and strains on the surface of the specimens.

It was found that the fiber waviness in the composite material caused notable changes in the behavior of composites and that the experimental results were in good agreement with the predictions based on the constitutive model.

Appendix A: Plane-Stress Moduli

Plane-stress moduli in Eq. (11) are calculated as

$$\left(Q_{xx}^{**}\right)_l = \left(C_{11}^{**}\right)_l + \frac{\left(C_{13}^{**}\right)_l\left(C_{13}^{**}\right)_l\left(C_{55}^{**}\right)_l + \left(C_{15}^{**}\right)_l\left(C_{15}^{**}\right)_l\left(C_{33}^{**}\right)_l - 2\left(C_{13}^{**}\right)_l\left(C_{15}^{**}\right)_l\left(C_{35}^{**}\right)_l}{\left(C_{35}^{**}\right)_l\left(C_{35}^{**}\right)_l - \left(C_{33}^{**}\right)_l\left(C_{55}^{**}\right)_l}$$

$$\left(Q_{xy}^{**}\right)_l = \left(Q_{yx}^{**}\right)_l = \left(C_{12}^{**}\right)_l + \frac{\left(C_{13}^{**}\right)_l\left(C_{23}^{**}\right)_l\left(C_{55}^{**}\right)_l + \left(C_{15}^{**}\right)_l\left(C_{25}^{**}\right)_l\left(C_{33}^{**}\right)_l - \left(C_{13}^{**}\right)_l\left(C_{25}^{**}\right)_l\left(C_{35}^{**}\right)_l - \left(C_{15}^{**}\right)_l\left(C_{23}^{**}\right)_l\left(C_{35}^{**}\right)_l}{\left(C_{35}^{**}\right)_l\left(C_{35}^{**}\right)_l - \left(C_{33}^{**}\right)_l\left(C_{55}^{**}\right)_l}$$

$$\left(Q_{yy}^{**}\right)_l = \left(C_{22}^{**}\right)_l + \frac{\left(C_{23}^{**}\right)_l\left(C_{23}^{**}\right)_l\left(C_{55}^{**}\right)_l + \left(C_{25}^{**}\right)_l\left(C_{25}^{**}\right)_l\left(C_{33}^{**}\right)_l - 2\left(C_{23}^{**}\right)_l\left(C_{25}^{**}\right)_l\left(C_{35}^{**}\right)_l}{\left(C_{35}^{**}\right)_l\left(C_{35}^{**}\right)_l - \left(C_{33}^{**}\right)_l\left(C_{55}^{**}\right)_l}$$

$$\left(Q_{ss}^{**}\right)_l = \left(C_{66}^{**}\right)_l - \frac{\left(C_{46}^{**}\right)_l\left(C_{46}^{**}\right)_l}{\left(C_{44}^{**}\right)_l} \tag{A1}$$

Appendix B: Differential Compliances

The differential compliances in Eq. (22) are calculated as

$$\left(\overline{S_{11}^{d***}}\right)_l = S_{11}I_1 + (2S_{13} + S_{55})I_3 + S_{33}I_5 + 2(\sigma_{xx})_l(S_{111}I_9 + S_{333}I_{13}) + 3(\sigma_{xx})_l^2(S_{1111}I_9 + S_{3333}I_{18} + S_{5555}I_{16}) \tag{B1}$$

where

$$I_1 = \frac{1 + c_l/2}{(c_l + 1)^{\frac{3}{2}}}, \qquad I_3 = \frac{c_l/2}{(c_l + 1)^{\frac{3}{2}}}$$

$$I_5 = 1 - \frac{1 + 3c_l/2}{(c_l + 1)^{\frac{3}{2}}}, \qquad I_9 = \frac{1 + c_l + 3c_l^2/8}{(c_l + 1)^{\frac{5}{2}}}$$

$$I_{13} = 1 - \frac{1 + 5c_l/2 + 15c_l^2/8}{(c_l + 1)^{\frac{5}{2}}}, \qquad I_{16} = \frac{3c_l^2/8 + c_l^3/16}{(c_l + 1)^{\frac{7}{2}}}$$

$$I_{18} = 1 - \frac{1 + 7c_l/2 + 35c_l^2/8 + 35c_l^3/16}{(c_l + 1)^{\frac{7}{2}}}$$

$$\left(\overline{S_{13}^{d***}}\right)_l = (S_{11} + S_{33} - S_{55})I_3 + S_{13}I_2 + 2(\sigma_{xx})_l(S_{111}I_{10} + S_{333}I_{12}) + 3(\sigma_{xx})_l^2(S_{1111}I_{15} + S_{3333}I_{17} - S_{5555}I_{16}) \tag{B2}$$

where

$$I_2 = 1 - \frac{c_1}{(c_l + 1)^{\frac{3}{2}}}, \qquad I_{10} = \frac{c_l/2 + c_l^2/8}{(c_l + 1)^{\frac{5}{2}}}$$

$$I_{12} = \frac{3c_l^2/8}{(c_l + 1)^{\frac{5}{2}}}, \qquad I_{15} = \frac{c_l/2 + c_l^2/4 + c_l^3/16}{(c_l + 1)^{\frac{7}{2}}}$$

$$I_{17} = \frac{5c_l^3/16}{(c_l + 1)^{\frac{7}{2}}}$$

where c_l is the same expression as Eq. (16).

The differential Young's modulus in Eq. (21) is calculated as

$$\left(\overline{E_x^{d***}}\right)_l = 1\Big/\left(\overline{S_{11}^{d***}}\right)_l \tag{B3}$$

Acknowledgment

The authors are grateful for the support provided by Brain Korea 21 from the Korea Research Foundation.

References

[1] Shuart, M. J., "Failure of Compression-Loaded Multi-Directional Composite Laminates," *AIAA Journal*, Vol. 27, No. 9, 1989, pp. 1274–1279.

[2] Bogetti, T. A., Gillespie, J. W., Jr., and Lamontia, M. A., "Influence of Ply Waviness with Nonlinear Shear on the Stiffness and Strength Reduction of Composite Laminates," *Mechanics of Composite Materials: Nonlinear*

Effects, AMD-Vol. 159, American Society of Mechanical Engineers, Fairfield, NJ, 1993, pp. 163–172.

[3]Telegadas, H. K., and Hyer, M. W., "The Influence of Layer Waviness on the Stress State in Hydrostatically Loaded Cylinders: Failure Prediction," *Journal of Reinforced Plastics and Composites*, Vol. 11, No. 2, 1992, pp. 127–145.

[4]Chou, T.-W., and Takahashi, K., "Non-Linear Elastic Behavior of Flexible Fibre Composites," *Composites*, Vol. 18, No. 1, 1987, pp. 25–33.

[5]Hsiao, H. M., and Daniel, I. M., "Nonlinear Elastic Behavior of Unidirectional Composites with Fiber Waviness Under Compressive Loading," *Journal of Engineering Materials and Technology*, Vol. 118, No. 4, 1996, pp. 561–570.

[6]Hsiao, H. M., and Daniel, I. M., "Effect of Fiber Waviness on Stiffness and Strength Reduction of Unidirectional Composites Under Compressive Loading," *Composites Science and Technology*, Vol. 56, No. 5, 1996, pp. 581–593.

[7]Hsiao, H. M., and Daniel, I. M., "Elastic Properties of Composites with Fiber Waviness," *Composites*, Vol. 27A, No. 10, 1996, pp. 931–941.

[8]Hsiao, H. M., Wooh, S. C., and Daniel, I. M., "Fabrication Methods for Unidirectional and Crossply Composites with Fiber Waviness," *Journal of Advanced Materials*, Vol. 26, No. 2, 1995, pp. 19–26.

A. M. Waas
Associate Editor